ACS OMEGA

http://pubs.acs.org/journal/acsodf

Article

Simple Solvent Treatment Enabled Improved PEDOT:PSS Performance toward Highly Efficient Binary Organic Solar Cells

Shasha Shi,[§] Yiwen Hou,[§] Tao Yang,*[,§] Ciyuan Huang,* Shangfei Yao, Chenfu Zhao, Yudie Liu, Ziyang Zhang, Tao Liu,* and Bingsuo Zou*

Cite This: *ACS Omega* 2022, 7, 41789−41795

Read Online

ACCESS | Metrics & More | Article Recommendations | Supporting Information

ABSTRACT: PEDOT:PSS is the most popular hole-transporting material (HTM) for conventional structural organic solar cell (OSC) devices, whose performance is of great importance for realizing high power conversion efficiency (PCE). However, its performance in OSC devices has been continuously challenged by various replacing materials and different doping strategies, for better conductivity, work function, and surface property. Here, we report a simple dopant-free method to tune the phase separation of the PEDOT:PSS layer, which results in better charge transport and extraction in devices. Specifically, high PCEs for binary polymer-small-molecule (>18%) and polymer−polymer (>17%) systems are simultaneously achieved. This work engineeringly provides encouraging improvement for OSC device performance with easy modification and scientifically offers insights into tuning the property of the PEDOT:PSS layer.

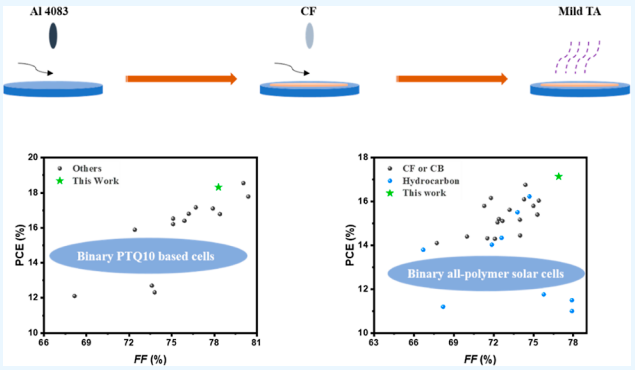

INTRODUCTION

Organic solar cell (OSC) technology, as a promising type of photovoltaic (PV), shall be readily prepared for further commercialization once the device performance appeals the market's requirement, which mainly relies on the quality of the active layer and charge transport layer.[1−12] By optimizing both of them, the power conversion efficiency (PCE), key factor of device performance, has reached 19% in several cases.[13−21] These exciting progresses usually require tremendous chemistry input or complex device engineering, so some simple yet effective ways to optimize the cast layers for OSCs are desired.

Compared with active layer optimization, the efforts made in the interlayer, both hole- and electron-transporting layer, are clearly less in recent years, although it is also an effective way for pursuing state-of-the-art PCEs.[22−32] Moreover, more research studies focus on the electron-transporting material (ETM) than hole-transporting material (HTM) because the universally applied PEDOT:PSS is easy to manipulate during the fabrication and can afford decent efficiency though its conductivity, and work function (WF) and surface morphology are moderate. Compared with those studies of finding replacing materials,[33] or applying dopants,[34] a simple modification without any more material input is advantageous for cost control. In previous studies, the phase segregation of PEDOT and PSS in the film was found to be an important factor in determining the performance, and it was found that thermal stress assists in smoothing the surface, which leads to suppressed device efficiency fluctuation and boosted short-circuit current density (J_{SC}).[35] Moreover, increasing the annealing temperature results in a smooth surface but breaks the inner packing and molecule composition, so pursuing a more uniform surface requires some other methods.

Herein, we report a simple solvent treatment on freshly cast PEDOT:PSS before the thermal annealing, which can tune the surface morphology, that is, phase distribution, thus enabling improved PCE for the corresponding devices. The control devices are composed of simply cast and annealed PEDOT:PSS films, and the target ones are with chloroform (CF)-modified films. The insoluble PEDOT and PSS phase can be moved by CF during spinning and then a tuned composition distribution, which realizes a more uniform surface after thermal annealing. Consequently, the corresponding device performances are promoted for three representative binary systems: PM6:BTP-2FThCl, PTQ10:m-BTP-PhC6, and PM6:PY-IT.[36−40] Specifically, 18.31 and 17.14% are at the leading level of the binary OSCs and hydrocarbon solvent-processed all-polymer solar cells, respectively. This research proposes a simple yet effective way to improve the

Received: September 24, 2022
Accepted: October 26, 2022
Published: November 3, 2022

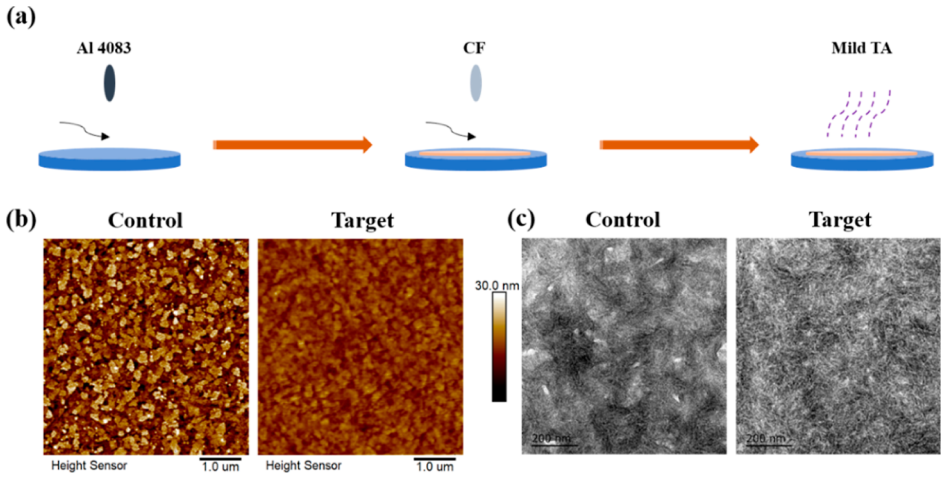

Figure 1. (a) PEDOT:PSS layer fabrication. (b) AFM and (c) TEM images of control and target films.

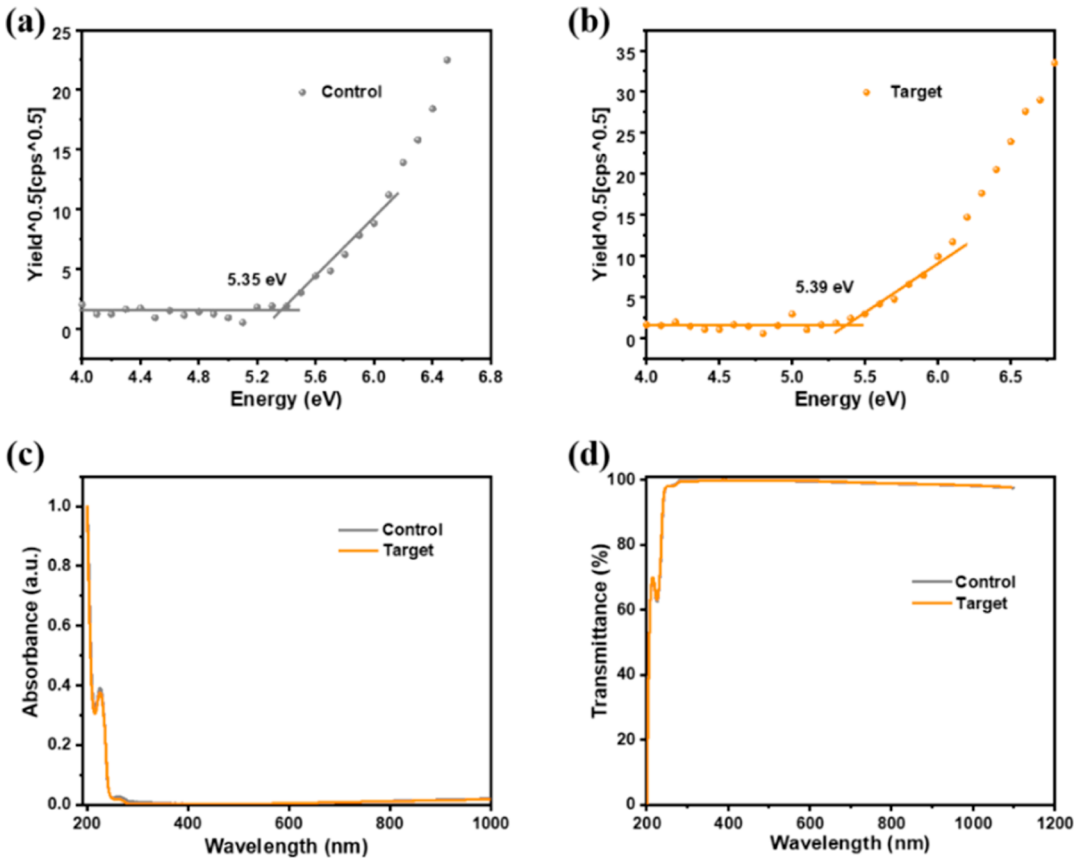

Figure 2. PESA results of the (a) control and (b) target. (c) Absorption and (d) transmission of the control and target.

PEDOT:PSS layer's performance by no further chemistry input.

RESULTS AND DISCUSSION

The operation of PEDOT:PSS layer modification is displayed in Figure 1a. Before thermal annealing (TA) processing, the just-cast PEDOT:PSS (Hareus Al 4083) film is rinsed with CF, one of those orthogonal solvents for the layer, which can endow the film with a different phase distribution after spinning without dissolving or breaking the film. Afterward, the TA procedure is applied. This is a simple modification of the PEDOT:PSS film without using dopants or synthetic methods, but effectively changing the surface morphology. Although CF cannot dissolve the film, it moves the particles during the high-speed spinning so that a tuned composition distribution can be achieved, which affords the chance of reaching further suppressed phase separation.

The morphology tuning difference of the surface modification between the control and target is compared by atomic force microscopy (AFM) height images and transmission electron microscopy (TEM) images, as shown in Figure 1b,c.[41−43] The calculated surface roughness values of the control and target are 5.19 and 2.86 nm, respectively. The results are consistent with the guess. Both the technology-

https://doi.org/10.1021/acsomega.2c06181
ACS Omega 2022, 7, 41789−41795

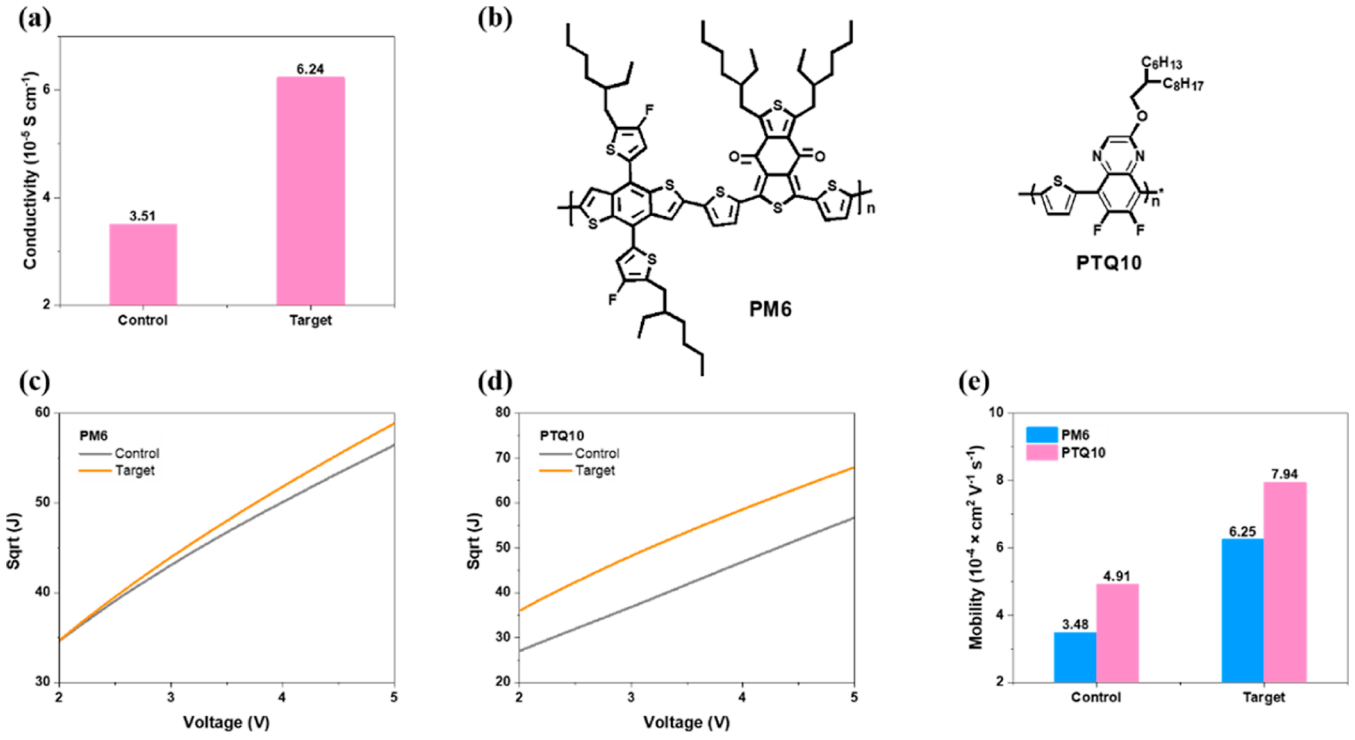

Figure 3. (a) Conductivity. (b) Chemical Structure of PM6 and PTQ10. The hole-only device results based on two films for (c) PM6 and (d) PTQ10. (e) Summarized mobility values.

captured images show that the modified target contains a more sophisticated nanofiber structure, smoother surface, and suppressed phase separation.

Then, we turn to investigate the morphology variation's impact on the HTM layer's basic properties. The WF values of them are determined by photoelectron spectroscopy in air (PESA) measurements upon the prepared films. As a result, the WF of the target film is improved from 5.35 to 5.38 eV compared to the unmodified one. Based on previous reports, properly enhanced WF of the PEDOT:PSS layer is friendly for boosting photovoltaic performance.[44−47] Besides, the transmission property of the films has been studied too. The general profiles of two films are nearly identical. The abovementioned data are presented in Figure 2. Then, the conductivity of the control is 3.51×10^{-5} S cm^{-1}, while that of the target is 6.24×10^{-5} S cm^{-1} (Figure 3a), according to the results of the four-point probe method. The significantly improved conductivity of the HTM-based layer is beneficial for charge extraction, and thus, better photovoltaic parameters such as open-circuit voltage (V_{OC}), J_{SC}, and fill factor (FF) are obtained.

Furthermore, we evaluate the charge transport property of diode devices with the control or target, using two popular p-type polymer materials (PM6 and PTQ10; Figure 3b) as the studying object.[48−50] The hole-only devices are fabricated based on the structure of ITO/control or target PEDOT:PSS/PM6 or PTQ10/MoO_3/Ag. The data analysis is enabled by Mott−Gurney relationship (details in the Supporting Information) where linear fitting can be carried out between applied voltage and square value of current density.[51] The curves are shown in Figure 3c,d, and the calculated results are listed in Figure 3e. It reveals that the modified HTM layer can promote the global hole transport in the photodiode devices, which is a positive signal for boosting FF.

Then, we use three different binary OSC combinations to investigate the PEDOT:PSS flattening modification's effect of promoting the photovoltaic performance, for which the device structure is ITO/control or target/active layer/ZrAcAc/Al. The recipes for active layer processing follow the former studies (note that PM6:PY-IT is dissolved by non-halogenated solvent o-XY).[36,37,51−53] The chemical structures of the acceptors are shown in Figure 4a. Their current density versus voltage ($J-V$) characteristics are plotted in Figure 4b, with extracted parameters summarized in Table 1. The device efficiency of PTQ10:m-BTP-PhC6 binary OSCs is increased from 17.56 to 18.31%, which is among the highest levels for PTQ10 (low-cost polymer donor)-composed binary devices. The performance enhancement benefits from V_{OC}, J_{SC}, and FF, as expected before. On the other hand, the solar cell based on PM6:BTP-2F-ThCl can achieve an efficiency of 17.70%, also outperforming the counterparts. At last, a 17.14% PCE is gained here due to the better HTM layer, which is one of the best values for non-halogenated solvent-treated binary all-polymer solar cells.[54−63]

The brackets contain averages and standard errors of PCEs based on at least 20 devices. Integrated values are behind the slashes.

Furthermore, the external quantum efficiency spectra of them are measured to assure the performance credibility. The integrated values are shown in Table 1 too. Accordingly, the errors are controlled to be smaller than 3%. Overall, the target type devices are all better than controls, indicating the effect and significance of this economic and simple modification method.

At last, the stability of devices based on control and target films is evaluated, shown in Figure 4d. It is reasonable that simple solvent treatment does not exhibit much change in this issue, since the chemical composition of the PEDOT:PSS layer

https://doi.org/10.1021/acsomega.2c06181
ACS Omega 2022, 7, 41789−41795

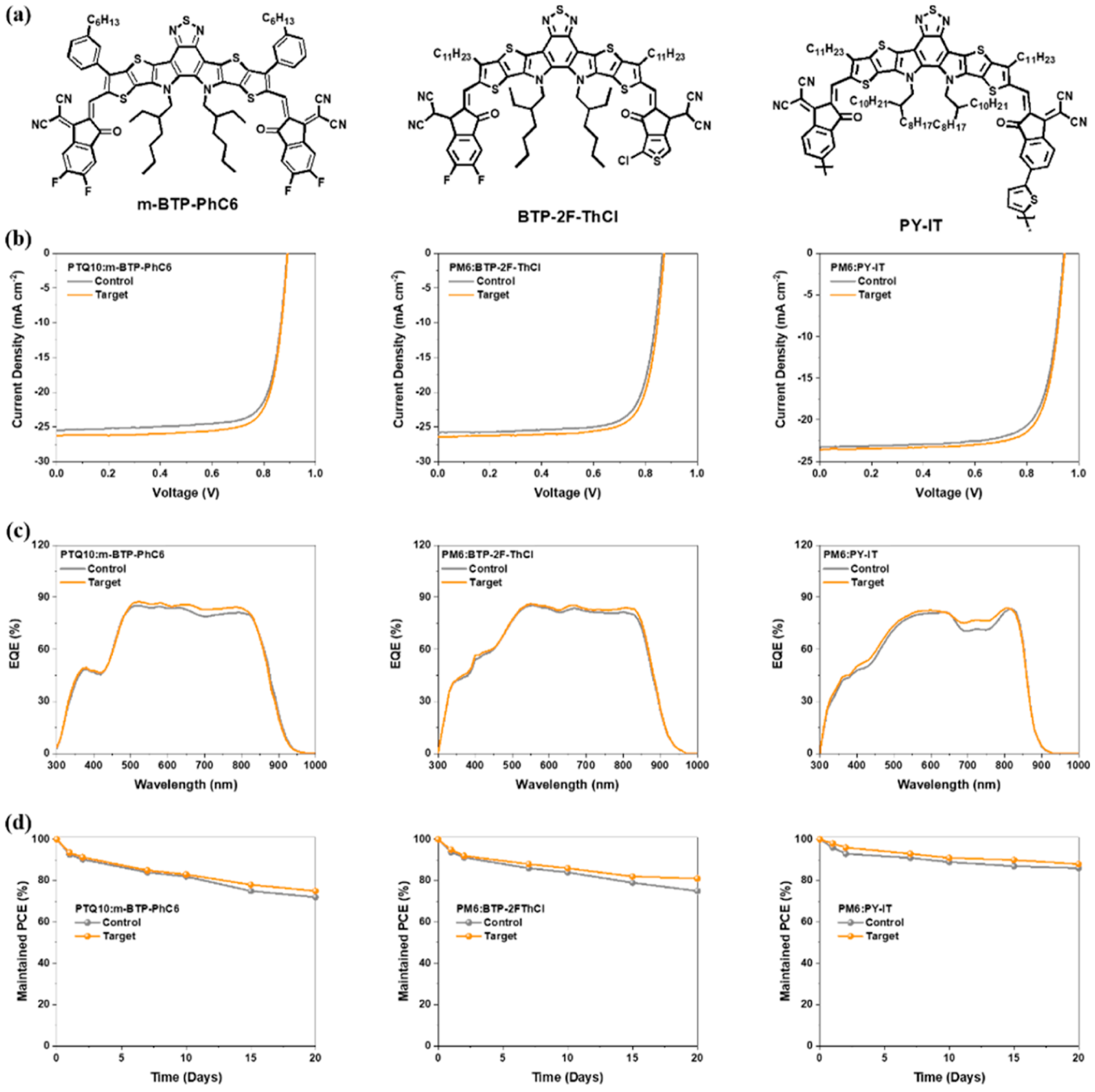

Figure 4. (a) Chemical structures of acceptor materials: *m*-BTP-PhC6, BTP-2F-ThCl, and PY-IT. (b) *J*−*V* characteristics of binary systems PTQ10:m-BTP-PhC6, PM6:BTP-2F-ThCl, and PM6:PY-IT. (c) Corresponding EQE spectra. (d) Shelf-like stability of the encapsulated devices in a nitrogen atmosphere.

Table 1. Device Performances

systems	V_{OC} (V)	J_{SC} (mA cm^{-2})	FF (%)	PCE (%)
		PTQ10:m-BTP-PhC6		
control	0.890	25.53/25.19	77.3	17.56 (17.22 ± 0.25)
target	0.891	26.25/25.69	78.3	18.31 (18.13 ± 0.17)
		PM6:BTP-2F-ThCl		
control	0.865	25.83/25.40	76.2	17.03 (16.78 ± 0.24)
target	0.872	26.46/25.94	76.7	17.70 (17.40 ± 0.20)
		PM6:PY-IT		
control	0.942	23.29/22.82	75.3	16.52 (16.31 ± 0.22)
target	0.945	23.57/23.50	76.9	17.14 (16.96 ± 0.19)

is still the same. All three groups of devices show very close storage stability, and the controls are slightly higher, indicating this strategy's effectiveness in promoting the comprehensive device performance.

In addition to the improvement of HTL performance, the change in free energy for the processed surface would also tune the vertical phase segregation, as mentioned by some previous papers, which could also contribute to enhanced device efficiency.[64] Although the surface free energy is hard to determine for PEDOT:PSS, this possible explanation deserves our discussion.

https://doi.org/10.1021/acsomega.2c06181
ACS Omega 2022, 7, 41789−41795

CONCLUSIONS

In summary, we apply an orthogonal solvent of the PEDOT:PSS layer, which succeeded in dragging the composition during the spinning and offered a more ideal starting point of surface morphology before the thermal annealing. As a result, a smoother surface can be achieved, and then, much improved conductivity and device mobility (also properly enhanced WF) can be obtained. This variation enables a universal efficiency enhancement in different photovoltaic systems, that is, three binary OSCs including state-of-the-art efficiency of all-polymer solar cells processed from the non-halogenated solvent.

ASSOCIATED CONTENT

Supporting Information

The Supporting Information is available free of charge at https://pubs.acs.org/doi/10.1021/acsomega.2c06181.

Device fabrication and characterization and thin-film characterization (PDF)

AUTHOR INFORMATION

Corresponding Authors

Tao Yang − *Julong College, Shenzhen Technology University, Shenzhen 518118, China;* orcid.org/0000-0001-8216-0574; Email: yangtao@sztu.edu.cn

Ciyuan Huang − *Guangxi Key Lab of Processing for Nonferrous Metals and Featured Materials and Key Lab of New Processing Technology for Nonferrous Metals and Materials, Ministry of Education; School of Resources, Environments and Materials, Guangxi University, Nanning 530004, China*; Email: huangciyuangxu@sina.com

Tao Liu − *Guangxi Key Lab of Processing for Nonferrous Metals and Featured Materials and Key Lab of New Processing Technology for Nonferrous Metals and Materials, Ministry of Education; School of Resources, Environments and Materials, Guangxi University, Nanning 530004, China;* orcid.org/0000-0001-6017-0827; Email: liutaozhx@gxu.edu.cn

Bingsuo Zou − *Guangxi Key Lab of Processing for Nonferrous Metals and Featured Materials and Key Lab of New Processing Technology for Nonferrous Metals and Materials, Ministry of Education; School of Resources, Environments and Materials, Guangxi University, Nanning 530004, China;* orcid.org/0000-0003-4561-4711; Email: zoubs@gxu.edu.cn

Authors

Shasha Shi − *Julong College, Shenzhen Technology University, Shenzhen 518118, China; Guangxi Key Lab of Processing for Nonferrous Metals and Featured Materials and Key Lab of New Processing Technology for Nonferrous Metals and Materials, Ministry of Education; School of Resources, Environments and Materials, Guangxi University, Nanning 530004, China*

Yiwen Hou − *Julong College, Shenzhen Technology University, Shenzhen 518118, China*

Shangfei Yao − *Guangxi Key Lab of Processing for Nonferrous Metals and Featured Materials and Key Lab of New Processing Technology for Nonferrous Metals and Materials, Ministry of Education; School of Resources, Environments and Materials, Guangxi University, Nanning 530004, China*

Chenfu Zhao − *Guangxi Key Lab of Processing for Nonferrous Metals and Featured Materials and Key Lab of New Processing Technology for Nonferrous Metals and Materials, Ministry of Education; School of Resources, Environments and Materials, Guangxi University, Nanning 530004, China*

Yudie Liu − *Guangxi Key Lab of Processing for Nonferrous Metals and Featured Materials and Key Lab of New Processing Technology for Nonferrous Metals and Materials, Ministry of Education; School of Resources, Environments and Materials, Guangxi University, Nanning 530004, China*

Ziyang Zhang − *Guangxi Key Lab of Processing for Nonferrous Metals and Featured Materials and Key Lab of New Processing Technology for Nonferrous Metals and Materials, Ministry of Education; School of Resources, Environments and Materials, Guangxi University, Nanning 530004, China*

Complete contact information is available at: https://pubs.acs.org/10.1021/acsomega.2c06181

Author Contributions

[§]S.S., Y.H., and T.Y. contributed equally.

Notes

The authors declare no competing financial interest.

ACKNOWLEDGMENTS

B.Z. thanks the Guangxi NSF project (2020GXNSFDA238004), the Scientific and Technological Bases and Talents of Guangxi (Guike AD21238027), and the special fund for "Guangxi Bagui Scholars". T.Y. appreciates the Shenzhen Key Laboratory of Marine Energies and Environmental Safety (ZDSYS20201215154000001) and Shenzhen Overseas Talent Project (NO. GDRC202102). T.L. appreciates the support of the Training Project of High-level Professional and Technical Talents of Guangxi University.

REFERENCES

(1) Su, Y.-W.; Lan, S.-C.; Wei, K.-H. Organic photovoltaics. *Mater Today* **2012**, *15*, 554−562.

(2) Facchetti, A. Polymer donor−polymer acceptor (all-polymer) solar cells. *Mater Today* **2013**, *16*, 123−132.

(3) Liu, Y.; Liu, B.; Ma, C.-Q.; Huang, F.; Feng, G.; Chen, H.; Hou, J.; Yan, L.; Wei, Q.; Luo, Q.; Bao, Q.; Ma, W.; Liu, W.; Li, W.; Wan, X.; Hu, X.; Han, Y.; Li, Y.; Zhou, Y.; Zou, Y.; Chen, Y.; Li, Y.; Chen, Y.; Tang, Z.; Hu, Z.; Zhang, Z.-G.; Bo, Z. Recent progress in organic solar cells (Part I material science). *Sci. China: Chem.* **2022**, *65*, 224−268.

(4) Meng, D.; Zheng, R.; Zhao, Y.; Zhang, E.; Dou, L.; Yang, Y. Near-Infrared Materials: The Turning Point of Organic Photovoltaics. *Adv. Mater.* **2022**, *34*, 2107330.

(5) Li, D.; Sun, C.; Yan, T.; Yuan, J.; Zou, Y. Asymmetric Non-Fullerene Small-Molecule Acceptors toward High-Performance Organic Solar Cells. *ACS Cent. Sci.* **2021**, *7*, 1787−1797.

(6) Zhou, K.; Xian, K.; Qi, Q.; Gao, M.; Peng, Z.; Liu, J.; Liu, Y.; Li, S.; Zhang, Y.; Geng, Y.; Ye, L. Unraveling the Correlations between Mechanical Properties, Miscibility, and Film Microstructure in All-Polymer Photovoltaic Cells. *Adv. Funct. Mater.* **2022**, *32*, 2201781.

(7) Chen, X.; Kan, B.; Kan, Y.; Zhang, M.; Jo, S. B.; Gao, K.; Lin, F.; Liu, F.; Peng, X.; Cao, Y.; Jen, A. K. Y. As-Cast Ternary Organic Solar Cells Based on an Asymmetric Side-Chains Featured Acceptor with Reduced Voltage Loss and 14.0% Efficiency. *Adv. Funct. Mater.* **2020**, *30*, 1909535.

(8) Ma, R.; Tao, Y.; Chen, Y.; Liu, T.; Luo, Z.; Guo, Y.; Xiao, Y.; Fang, J.; Zhang, G.; Li, X.; Guo, X.; Yi, Y.; Zhang, M.; Lu, X.; Li, Y.; Yan, H. Achieving 16.68% efficiency ternary as-cast organic solar cells. *Sci. China: Chem.* **2021**, *64*, 581−589.

(9) Chen, W.; Zhu, Y.; Xiu, J.; Chen, G.; Liang, H.; Liu, S.; Xue, H.; Birgersson, E.; Ho, J. W.; Qin, X.; Lin, J.; Ma, R.; Liu, T.; He, Y.; Ng, A. M.-C.; Guo, X.; He, Z.; Yan, H.; Djurišić, A. B.; Hou, Y. Monolithic perovskite/organic tandem solar cells with 23.6% efficiency enabled by reduced voltage losses and optimized interconnecting layer. *Nat. Energy* **2022**, *7*, 229−237.
(10) Fan, Q.; Ma, R.; Liu, T.; Yu, J.; Xiao, Y.; Su, W.; Cai, G.; Li, Y.; Peng, W.; Guo, T.; Luo, Z.; Sun, H.; Hou, L.; Zhu, W.; Lu, X.; Gao, F.; Moons, E.; Yu, D.; Yan, H.; Wang, E. High-performance all-polymer solar cells enabled by a novel low bandgap non-fully conjugated polymer acceptor. *Sci. China: Chem.* **2021**, *64*, 1380−1388.
(11) He, Y.; Li, N.; Heumüller, T.; Wortmann, J.; Hanisch, B.; Aubele, A.; Lucas, S.; Feng, G.; Jiang, X.; Li, W.; Bäuerle, P.; Brabec, C. J. Industrial viability of single-component organic solar cells. *Joule* **2022**, *6*, 1160−1171.
(12) Jiang, Y.; Dong, X.; Sun, L.; Liu, T.; Qin, F.; Xie, C.; Jiang, P.; Hu, L.; Lu, X.; Zhou, X.; Meng, W.; Li, N.; Brabec, C. J.; Zhou, Y. An alcohol-dispersed conducting polymer complex for fully printable organic solar cells with improved stability. *Nat. Energy* **2022**, *7*, 352−359.
(13) Ma, R.; Yan, C.; Yu, J.; Liu, T.; Liu, H.; Li, Y.; Chen, J.; Luo, Z.; Tang, B.; Lu, X.; Li, G.; Yan, H. High-Efficiency Ternary Organic Solar Cells with a Good Figure-of-Merit Enabled by Two Low-Cost Donor Polymers. *ACS Energy Lett.* **2022**, *7*, 2547−2556.
(14) Zhu, L.; Zhang, M.; Xu, J.; Li, C.; Yan, J.; Zhou, G.; Zhong, W.; Hao, T.; Song, J.; Xue, X.; Zhou, Z.; Zeng, R.; Zhu, H.; Chen, C.-C.; MacKenzie, R. C. I.; Zou, Y.; Nelson, J.; Zhang, Y.; Sun, Y.; Liu, F. Single-junction organic solar cells with over 19% efficiency enabled by a refined double-fibril network morphology. *Nat. Mater.* **2022**, *21*, 656−663.
(15) Wei, Y.; Chen, Z.; Lu, G.; Yu, N.; Li, C.; Gao, J.; Gu, X.; Hao, X.; Lu, G.; Tang, Z.; Zhang, J.; Wei, Z.; Zhang, X.; Huang, H. Binary Organic Solar Cells Breaking 19% via Manipulating Vertical Component Distribution. *Adv. Mater.* **2022**, *34*, 2204718.
(16) Zheng, Z.; Wang, J.; Bi, P.; Ren, J.; Wang, Y.; Yang, Y.; Liu, X.; Zhang, S.; Hou, J. Tandem Organic Solar Cell with 20.2% Efficiency. *Joule* **2022**, *6*, 171−184.
(17) Ma, R.; Yan, C.; Fong, P. W.-K.; Yu, J.; Liu, H.; Yin, J.; Huang, J.; Lu, X.; Yan, H.; Li, G. In situ and ex situ investigations on ternary strategy and co-solvent effects towards high-efficiency organic solar cells. *Energy Environ. Sci.* **2022**, *15*, 2479−2488.
(18) Zhan, L.; Yin, S.; Li, Y.; Li, S.; Chen, T.; Sun, R.; Min, J.; Zhou, G.; Zhu, H.; Chen, Y.; Fang, J.; Ma, C.-Q.; Xia, X.; Lu, X.; Qiu, H.; Fu, W.; Chen, H. Multi-Phase Morphology with Enhanced Carrier Lifetime via Quaternary Strategy Enables High-Efficiency Thick-Film and Large-Area Organic Photovoltaics. *Adv. Mater.* **2022**, 2206269.
(19) Cui, Y.; Xu, Y.; Yao, H.; Bi, P.; Hong, L.; Zhang, J.; Zu, Y.; Zhang, T.; Qin, J.; Ren, J.; Chen, Z.; He, C.; Hao, X.; Wei, Z.; Hou, J. Single-Junction Organic Photovoltaic Cell with 19% Efficiency. *Adv. Mater.* **2021**, *33*, 2102420.
(20) Zhan, L.; Li, S.; Li, Y.; Sun, R.; Min, J.; Bi, Z.; Ma, W.; Chen, Z.; Zhou, G.; Zhu, H.; Shi, M.; Zuo, L.; Chen, H. Desired open-circuit voltage increase enables efficiencies approaching 19% in symmetric-asymmetric molecule ternary organic photovoltaics. *Joule* **2022**, *6*, 662−675.
(21) Li, Y.; Cai, Y.; Xie, Y.; Song, J.; Wu, H.; Tang, Z.; Zhang, J.; Huang, F.; Sun, Y. A facile strategy for third-component selection in non-fullerene acceptor-based ternary organic solar cells. *Energy Environ. Sci.* **2021**, *14*, 5009−5016.
(22) Lin, Y.; Firdaus, Y.; Isikgor, F. H.; Nugraha, M. I.; Yengel, E.; Harrison, G. T.; Hallani, R.; El-Labban, A.; Faber, H.; Ma, C.; Zheng, X.; Subbiah, A.; Howells, C. T.; Bakr, O. M.; McCulloch, I.; Wolf, S. D.; Tsetseris, L.; Anthopoulos, T. D. Self-Assembled Monolayer Enables Hole Transport Layer-Free Organic Solar Cells with 18% Efficiency and Improved Operational Stability. *ACS Energy Lett.* **2020**, *5*, 2935−2944.
(23) Ma, R.; Zeng, M.; Li, Y.; Liu, T.; Luo, Z.; Xu, Y.; Li, P.; Zheng, N.; Li, J.; Li, Y.; Chen, R.; Hou, J.; Huang, F.; Yan, H. Rational Anode Engineering Enables Progresses for Different Types of Organic Solar Cells. *Adv. Energy Mater.* **2021**, *11*, 2100492.
(24) Xu, H.; Yuan, F.; Zhou, D.; Liao, X.; Chen, L.; Chen, Y. Hole transport layers for organic solar cells: recent progress and prospects. *J. Mater. Chem. A* **2020**, *8*, 11478−11492.
(25) Ma, R.; Zhou, K.; Sun, Y.; Liu, T.; Kan, Y.; Xiao, Y.; Dela Peña, T. A.; Li, Y.; Zou, X.; Xing, Z.; Luo, Z.; Wong, K. S.; Lu, X.; Ye, L.; Yan, H.; Gao, K. Achieving high efficiency and well-kept ductility in ternary all-polymer organic photovoltaic blends thanks to two well miscible donors. *Matter* **2022**, *5*, 725−734.
(26) Meng, H.; Liao, C.; Deng, M.; Xu, X.; Yu, L.; Peng, Q. 18.77 % Efficiency Organic Solar Cells Promoted by Aqueous Solution Processed Cobalt(II) Acetate Hole Transporting Layer. *Angew. Chem., Int. Ed.* **2021**, *60*, 22554−22561.
(27) Zheng, Z.; Hu, Q.; Zhang, S.; Zhang, D.; Wang, J.; Xie, S.; Wang, R.; Qin, Y.; Li, W.; Hong, L.; Liang, N.; Liu, F.; Zhang, Y.; Wei, Z.; Tang, Z.; Russell, T. P.; Hou, J.; Zhou, H. A Highly Efficient Non-Fullerene Organic Solar Cell with a Fill Factor over 0.80 Enabled by a Fine-Tuned Hole-Transporting Layer. *Adv. Mater.* **2018**, *30*, 1801801.
(28) Zeng, M.; Wang, X.; Ma, R.; Zhu, W.; Li, Y.; Chen, Z.; Zhou, J.; Li, W.; Liu, T.; He, Z.; Yan, H.; Huang, F.; Cao, Y. Dopamine Semiquinone Radical Doped PEDOT:PSS: Enhanced Conductivity, Work Function and Performance in Organic Solar Cells. *Adv. Energy Mater.* **2020**, *10*, 2000743.
(29) Lin, Y.; Adilbekova, B.; Firdaus, Y.; Yengel, E.; Faber, H.; Sajjad, M.; Zheng, X.; Yarali, E.; Seitkhan, A.; Bakr, O. M.; El-Labban, A.; Schwingenschlögl, U.; Tung, V.; McCulloch, I.; Laquai, F.; Anthopoulos, T. D. 17% Efficient Organic Solar Cells Based on Liquid Exfoliated WS2 as a Replacement for PEDOT:PSS. *Adv. Mater.* **2019**, *31*, 1902965.
(30) Yang, T.; Yao, S.; Liu, T.; Huang, B.; Xiao, Y.; Liu, H.; Lu, X.; Zou, B. Tailoring the Morphology's Microevolution for Binary All-Polymer Solar Cells Processed by Aromatic Hydrocarbon Solvent with 16.22% Efficiency. *ACS Appl. Mater. Interfaces* **2022**, *14*, 29956−29963.
(31) Kang, Q.; Zheng, Z.; Zu, Y.; Liao, Q.; Bi, P.; Zhang, S.; Yang, Y.; Xu, B.; Hou, J. n-doped inorganic molecular clusters as a new type of hole transport material for efficient organic solar cells. *Joule* **2021**, *5*, 646−658.
(32) Wang, J.; Zheng, Z.; Zhang, D.; Zhang, J.; Zhou, J.; Liu, J.; Xie, S.; Zhao, Y.; Zhang, Y.; Wei, Z.; Hou, J.; Tang, Z.; Zhou, H. Regulating Bulk-Heterojunction Molecular Orientations through Surface Free Energy Control of Hole-Transporting Layers for High-Performance Organic Solar Cells. *Adv. Mater.* **2019**, *31*, 1806921.
(33) Kang, Q.; Liao, Q.; Yang, C.; Yang, Y.; Xu, B.; Hou, J. A New PEDOT Derivative for Efficient Organic Solar Cell with a Fill Factor of 0.80. *Adv. Energy Mater.* **2022**, *12*, 2103892.
(34) Liu, T.; Sun, L.; Dong, X.; Jiang, Y.; Wang, W.; Xie, C.; Zeng, W.; Liu, Y.; Qin, F.; Hu, L.; Zhou, Y. Low-Work-Function PEDOT Formula as a Stable Interlayer and Cathode for Organic Solar Cells. *Adv. Funct. Mater.* **2021**, *31*, 2107250.
(35) Kim, Y.; Ballantyne, A. M.; Nelson, J.; Bradley, D. D. C. Effects of thickness and thermal annealing of the PEDOT:PSS layer on the performance of polymer solar cells. *Org. Electron.* **2009**, *10*, 205−209.
(36) Luo, Z.; Ma, R.; Liu, T.; Yu, J.; Xiao, Y.; Sun, R.; Xie, G.; Yuan, J.; Chen, Y.; Chen, K.; Chai, G.; Sun, H.; Min, J.; Zhang, J.; Zou, Y.; Yang, C.; Lu, X.; Gao, F.; Yan, H. Fine-Tuning Energy Levels via Asymmetric End Groups Enables Polymer Solar Cells with Efficiencies over 17%. *Joule* **2020**, *4*, 1236−1247.
(37) Chai, G.; Chang, Y.; Zhang, J.; Xu, X.; Yu, L.; Zou, X.; Li, X.; Chen, Y.; Luo, S.; Liu, B.; Bai, F.; Luo, Z.; Yu, H.; Liang, J.; Liu, T.; Wong, K. S.; Zhou, H.; Peng, Q.; Yan, H. Fine-tuning of side-chain orientations on nonfullerene acceptors enables organic solar cells with 17.7% efficiency. *Energy Environ. Sci.* **2021**, *14*, 3469−3479.
(38) Luo, Z.; Liu, T.; Ma, R.; Xiao, Y.; Zhan, L.; Zhang, G.; Sun, H.; Ni, F.; Chai, G.; Wang, J.; Zhong, C.; Zou, Y.; Guo, X.; Lu, X.; Chen, H.; Yan, H.; Yang, C. Precisely Controlling the Position of Bromine on the End Group Enables Well-Regular Polymer Acceptors for All-

https://doi.org/10.1021/acsomega.2c06181
ACS Omega 2022, 7, 41789−41795

Polymer Solar Cells with Efficiencies over 15%. *Adv. Mater.* **2020**, *32*, 2005942.
(39) Ma, R.; Yu, J.; Liu, T.; Zhang, G.; Xiao, Y.; Luo, Z.; Chai, G.; Chen, Y.; Fan, Q.; Su, W.; Li, G.; Wang, E.; Lu, X.; Gao, F.; Tang, B.; Yan, H. All-polymer solar cells with over 16% efficiency and enhanced stability enabled by compatible solvent and polymer additives. *Aggregate* **2022**, *3*, No. e58.
(40) Liu, T.; Yang, T.; Ma, R.; Zhan, L.; Luo, Z.; Zhang, G.; Li, Y.; Gao, K.; Xiao, Y.; Yu, J.; Zou, X.; Sun, H.; Zhang, M.; Dela Peña, T. A.; Xing, Z.; Liu, H.; Li, X.; Li, G.; Huang, J.; Duan, C.; Wong, K. S.; Lu, X.; Guo, X.; Gao, F.; Chen, H.; Huang, F.; Li, Y.; Li, Y.; Cao, Y.; Tang, B.; Yan, H. 16% efficiency all-polymer organic solar cells enabled by a finely tuned morphology via the design of ternary blend. *Joule* **2021**, *5*, 914−930.
(41) Pei, S.; Xiong, X.; Zhong, W.; Xue, X.; Zhang, M.; Hao, T.; Zhang, Y.; Liu, F.; Zhu, L. Highly Efficient Organic Solar Cells Enabled by the Incorporation of a Sulfonated Graphene Doped PEDOT:PSS Interlayer. *ACS Appl. Mater. Interfaces* **2022**, *14*, 34814−34821.
(42) Xiong, X.; Xue, X.; Zhang, M.; Hao, T.; Han, Z.; Sun, Y.; Zhang, Y.; Liu, F.; Pei, S.; Zhu, L. Melamine-Doped Cathode Interlayer Enables High-Efficiency Organic Solar Cells. *ACS Energy Lett.* **2021**, *6*, 3582−3589.
(43) Yao, J.; Ding, S.; Zhang, R.; Bai, Y.; Zhou, Q.; Meng, L.; Solano, E.; Steele, J. A.; Roeffaers, M. B. J.; Gao, F.; Zhang, Z.-G.; Li, Y. Fluorinated Perylene-diimides: Cathode Interlayers Facilitating Carrier Collection for High-Performance Organic Solar Cells. *Adv. Mater.* **2022**, *34*, 2203690.
(44) Tang, H.; Liu, Z.; Hu, Z.; Liang, Y.; Huang, F.; Cao, Y. Oxoammonium enabled secondary doping of hole transporting material PEDOT:PSS for high-performance organic solar cells. *Sci. China: Chem.* **2020**, *63*, 802−809.
(45) Guo, B.; Yin, Q.; Zhou, J.; Li, W.; Zhang, K.; Li, Y. Semiconductive Polymer-Doped PEDOT with High Work Function, Conductivity, Reversible Dispersion, and Application in Organic Solar Cells. *ACS Sustainable Chem. Eng.* **2019**, *7*, 8206−8214.
(46) Chiou, G.-C.; Lin, M.-W.; Lai, Y.-L.; Chang, C.-K.; Jiang, J.-M.; Su, Y.-W.; Wei, K.-H.; Hsu, Y.-J. Fluorene Conjugated Polymer/Nickel Oxide Nanocomposite Hole Transport Layer Enhances the Efficiency of Organic Photovoltaic Devices. *ACS Appl. Mater. Interfaces* **2017**, *9*, 2232−2239.
(47) Savagatrup, S.; Chan, E.; Renteria-Garcia, S. M.; Printz, A. D.; Zaretski, A. V.; O'Connor, T. F.; Rodriquez, D.; Valle, E.; Lipomi, D. J. Plasticization of PEDOT:PSS by Common Additives for Mechanically Robust Organic Solar Cells and Wearable Sensors. *Adv. Funct. Mater.* **2015**, *25*, 427−436.
(48) Zhang, M.; Guo, X.; Ma, W.; Ade, H.; Hou, J. A Large-Bandgap Conjugated Polymer for Versatile Photovoltaic Applications with High Performance. *Adv. Mater.* **2015**, *27*, 4655−4660.
(49) Ma, R.; Liu, T.; Luo, Z.; Guo, Q.; Xiao, Y.; Chen, Y.; Li, X.; Luo, S.; Lu, X.; Zhang, M.; Li, Y.; Yan, H. Improving open-circuit voltage by a chlorinated polymer donor endows binary organic solar cells efficiencies over 17%. *Sci. China: Chem.* **2020**, *63*, 325−330.
(50) Sun, C.; Pan, F.; Bin, H.; Zhang, J.; Xue, L.; Qiu, B.; Wei, Z.; Zhang, Z.-G.; Li, Y. A low cost and high performance polymer donor material for polymer solar cells. *Nat. Commun.* **2018**, *9*, 743.
(51) Huang, Y.-J.; Chen, H.-C.; Lin, H.-K.; Wei, K.-H. Doping ZnO Electron Transport Layers with MoS2 Nanosheets Enhances the Efficiency of Polymer Solar Cells. *ACS Appl. Mater. Interfaces* **2018**, *10*, 20196−20204.
(52) Ding, S.; Ma, R.; Yang, T.; Zhang, G.; Yin, J.; Luo, Z.; Chen, K.; Miao, Z.; Liu, T.; Yan, H.; Xue, D. Boosting the Efficiency of Non-fullerene Organic Solar Cells via a Simple Cathode Modification Method. *ACS Appl. Mater. Interfaces* **2021**, *13*, 51078−51085.
(53) Yang, T.; Yao, S.; Liu, T.; Huang, B.; Xiao, Y.; Liu, H.; Lu, X.; Zou, B. Tailoring the Morphology's Microevolution for Binary All-Polymer Solar Cells Processed by Aromatic Hydrocarbon Solvent with 16.22% Efficiency. *ACS Appl. Mater. Interfaces* **2022**, *14*, 29956−29963.
(54) Zhang, J.; Jia, T.; Tan, C.-H.; Zhang, K.; Ren, M.; Dong, S.; Xu, Q.; Huang, F.; Cao, Y. Nonhalogenated-Solvent-Processed High-Performance All-Polymer Solar Cell with Efficiency over 14%. *Sol. RRL* **2021**, *5*, 2100076.
(55) Zhu, L.; Zhong, W.; Qiu, C.; Lyu, B.; Zhou, Z.; Zhang, M.; Song, J.; Xu, J.; Wang, J.; Ali, J.; Feng, W.; Shi, Z.; Gu, X.; Ying, L.; Zhang, Y.; Liu, F. Aggregation-Induced Multilength Scaled Morphology Enabling 11.76% Efficiency in All-Polymer Solar Cells Using Printing Fabrication. *Adv. Mater.* **2019**, *31*, 1902899.
(56) Jin, L.; Ma, R.; Liu, H.; Xu, W.; Luo, Z.; Liu, T.; Su, W.; Li, Y.; Lu, R.; Lu, X.; Yan, H.; Tang, B. Z.; Yang, T. Boosting Highly Efficient Hydrocarbon Solvent-Processed All-Polymer-Based Organic Solar Cells by Modulating Thin-Film Morphology. *ACS Appl. Mater. Interfaces* **2021**, *13*, 34301−34307.
(57) Zhu, C.; Li, Z.; Zhong, W.; Peng, F.; Zeng, Z.; Ying, L.; Huang, F.; Cao, Y. Constructing a new polymer acceptor enabled non-halogenated solvent-processed all-polymer solar cell with an efficiency of 13.8%. *Chem. Commun.* **2021**, *57*, 935−938.
(58) Ding, S.; Ma, R.; Yang, T.; Zhang, G.; Yin, J.; Luo, Z.; Chen, K.; Miao, Z.; Liu, T.; Yan, H.; Xue, D. Boosting the Efficiency of Non-fullerene Organic Solar Cells via a Simple Cathode Modification Method. *ACS Appl. Mater. Interfaces* **2021**, *13*, 51078−51085.
(59) Ma, R.; Yang, T.; Xiao, Y.; Liu, T.; Zhang, G.; Luo, Z.; Li, G.; Lu, X.; Yan, H.; Tang, B. Air-Processed Efficient Organic Solar Cells from Aromatic Hydrocarbon Solvent without Solvent Additive or Post-Treatment: Insights into Solvent Effect on Morphology. *Energy Environ. Mater.* **2022**, *5*, 977−985.
(60) Zhang, J.; Huang, Q.; Zhang, K.; Jia, T.; Jing, J.; Chen, Y.; Li, Y.; Chen, Y.; Lu, X.; Wu, H.; Huang, F.; Cao, Y. Random Copolymerization Strategy Enables Non-Halogenated Solvent-Processed All-Polymer Solar Cells with High Efficiency over 17%. *Energy Environ. Sci.* **2022**, DOI: 10.1039/D2EE01996E.
(61) Hu, K.; Zhu, C.; Ding, K.; Qin, S.; Lai, W.; Du, J.; Zhang, J.; Wei, Z.; Li, X.; Zhang, Z.; Meng, L.; Ade, H.; Li, Y. Solid additive tuning of polymer blend morphology enables non-halogenated-solvent all-polymer solar cells with an efficiency of over 17%. *Energy Environ. Sci.* **2022**, *15*, 4157−4166.
(62) Jia, T.; Zhang, J.; Zhang, G.; Liu, C.; Tang, H.; Zhang, K.; Huang, F. Rationally regulating the terminal unit and copolymerization spacer of polymerized small-molecule acceptors for all-polymer solar cells with high open-circuit voltage over 1.10 V. *J. Mater. Chem. A* **2022**, *10*, 15932−15940.
(63) Song, J.; Li, Y.; Cai, Y.; Zhang, R.; Wang, S.; Xin, J.; Han, L.; Wei, D.; Ma, W.; Gao, F.; Sun, Y. Solid additive engineering enables high-efficiency and eco-friendly all-polymer solar cells. *Matter* **2022**, *5* (11), 4047−4059.
(64) Cheng, H.-W.; Raghunath, P.; Wang, K.-l.; Cheng, P.; Haung, T.; Wu, Q.; Yuan, J.; Lin, Y.-C.; Wang, H.-C.; Zou, Y.; Wang, Z.-K.; Lin, M. C.; Wei, K.-H.; Yang, Y. Potassium-Presenting Zinc Oxide Surfaces Induce Vertical Phase Separation in Fullerene-Free Organic Photovoltaics. *Nano Lett.* **2020**, *20*, 715−721.

https://doi.org/10.1021/acsomega.2c06181
ACS Omega 2022, 7, 41789−41795